Electronic Supplementary Information

Generation of Triplet Diradical from a Donor-Acceptor Cross Conjugate upon Acid-Induced Electron Transfer

Mats O. Sandberg, Osami Nagao, Zhikun Wu, Michio M. Matsushita, and Tadashi Sugawara*

Department of Basic Science, Graduate School of Arts & Sciences, The University of

Tokyo, Komaba, Meguro-ku, Tokyo 153-8902, JAPAN

e-mail: suga@pentacle.c.u-tokyo.ac.jp

Contents:

Sandberg, Sugawara *et al.*

Supplementary Information 1: Synthetic procedure of cross-conjugate **QA**

Preparative route to cross-conjugate molecule (**1**) is shown in Scheme below. N,N'-diacetyl-N-phenyl-*p*-phenylenediamine (**2**) was coupled with m-dibromobenzene using cupper iodide as a catalyst to afford bromoaniline derivertive (**3**), and the protecting groups of **3** were switched with BOC and it was coupled with *N,N*-dianisylanilino boric acid[1] by Suzuki coupling,[2] giving rise to the coupled product (**4**). Deprotection of the *p*-phenylenediamine unit of **4**, followed by oxidation with lead dioxide afforded cross-conjugate molecule **1** with the benzoquinone diimine unit,[3] in which both *E*- and *Z* isomers[4] are present. The proton NMR spectrum recorded at room temperature in a chloroform-*d* showed several poorly resolved aromatic peaks between 6.7 and 7.5 ppm vs. tetramethylsilane. The intensity ratio of the aromatic peaks and that of the methoxy groups was 25:6. Coupling patterns indicated by a ^{1}H-^{1}H COSY NMR spectrum were consistent with presence of the E and Z isomers of this molecule. FAB-MS using *m*-nitrobenzylalcohol as a matrix showed the molecular peak at 561.5 (calc. 561.68) as the largest peak for m/z > 400.
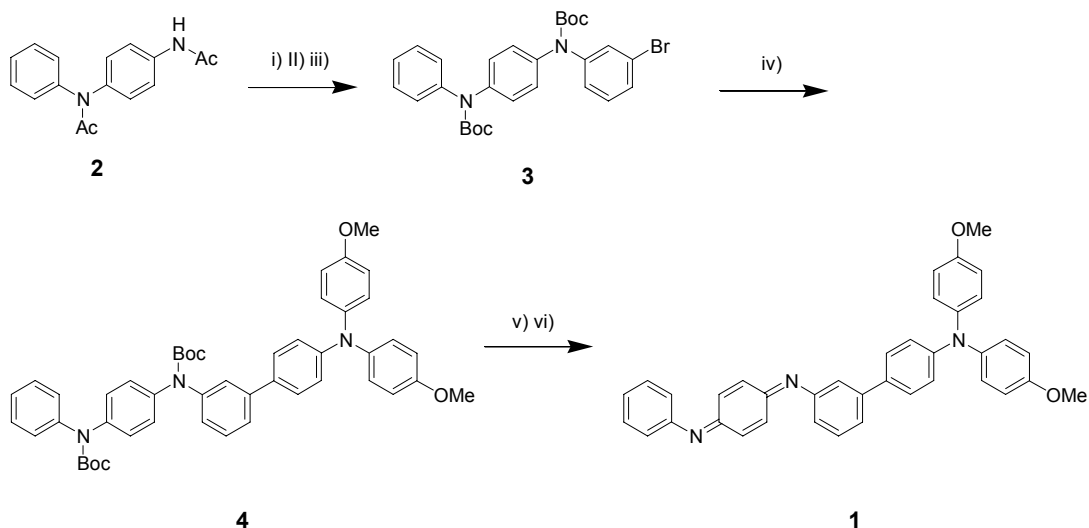
Scheme. Synthetic Procedure of the conjugate molecule **1**. i) *m*-Dibromobenzene, CuI, Ethoxyethylether, K_2CO_3; ii) NaOH aq, EtOH; iii) (BOC)$_2$O, 4-Dimethylaminopyridine; iv) N,N-Dianisyl-4-aminophenylboronic acid, Na_2CO_3 , Pd(PPh$_3$)$_4$; v) Me$_3$SiI, Et$_3$N, MeOH; vi) PbO$_2$, K$_2$CO$_3$.

References

1) Bushby, R. J., McGill, D. R., Ng, K. M., and Taylor, N. *J. Chem. Soc., Perkin Trans.* 2, **1997**, 1405.
2) Miyaura, N., Yanagi, T., and Suzuki, A. *Symth. Commun.*, **1981**, 513.
3) Wienk, M. M. and Janssen, R. A. J. *J. Am. Chem. Soc.,* 1996, **118**, 10626.
4) Sandberg, M. and Hjertberg, T. *Synth Met.,* 1989, **29**, E257.

Sandberg, Sugawara *et al.*

Supplementary Information 2: UV-Vis Spectra of **QA** upon titration with trifluoroacetic acid.

The change in the electronic structure of **QA** upon titration with trifluoroacetic acid (TFA) to the dichloromethane solution of **QA** was monitored by UV-Vis absorption spectroscopy as shown in figure below. An orange color solution of cross-conjugate **QA** in dichloromethane shows two absorption peaks at 305 and 442 nm, the former peak being characteristic to the benzoquinone diimine unit. Upon the addition of TFA to the dichloromethane solution of **QA** ([TFA]/[**QA**] < 0.5), a new absorption with the maximum at 550 nm increased in compensation with the decrease of the band at 305 nm, having an isosbestic point at 344 nm. The absorption at 550 nm was assigned to the mono-protonated species of **QA** at the benzoquinone diimine unit. When the ratio of [TFA]/[**QA**] became larger than 1.0, the red color of the solution turned to deep blue. Accompanied by the color change, a strong absorption band at 757 nm with a shoulder at 640 nm grew, exhibiting the isosbestic points at 567, 421, and 366 nm (Figure right below). Further addition of TFA did not cause any changes in the absorption spectrum. Since the band at 757 nm is similar to the cation radical of trianisyl amine, it is certain that the single electron transfer occurs from triarylamine to the doubly protonated quinodiimine unit at this stage.

As a reference compound of mono-protonated **QA,** mono-protnated diphenyl benzoquinodiime (**QI·H$^+$**) was generated by adding TFA to a dichloromethane solution of diphenyl benzoquinodiime (**QI**) in the ratio of [TFA] /[**QI**] = 1 :0.5. The solution showed the absorption band at 530 nm which was ascribed to **QI·H$^+$**. The result supports the above assignment.

a)   b)
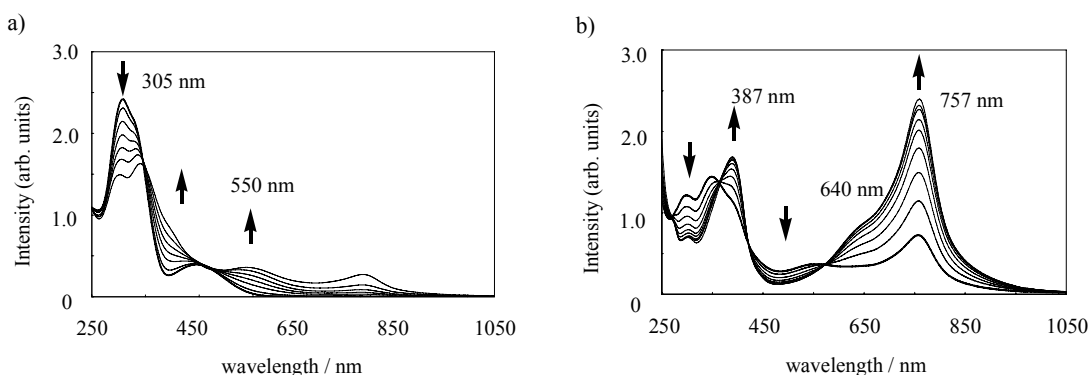
**Figure** UV-vis spectra of **QA** in dichloromethan solution titrated by trifluoroacetic acid (TFA). a) [TFA] / [**QA**] < 0.5. The isosbestic point was observed at 344 nm. b) [TFA] / [**QA**] > 1.0. Isosbestic points were observed at 366, 412, and 567 nm.

Sandberg, Sugawara *et al.*

Supplementary Information 3: ESR spectrum of $QA \cdot H_2^{2+}$ in a PVC matrix.

A polyvinylchloride (PVC) film containing **QA** was prepared by evaporation from their THF solution. The orange color of this film was turned out to be deep blue when the film was exposed to hydrogen chloride gas. ESR spectrum of the deep blue film at 60 K showed a broad peak centered around g = 2.0036 flanked by two shoulders separated by 4.1 mT.

1 mT
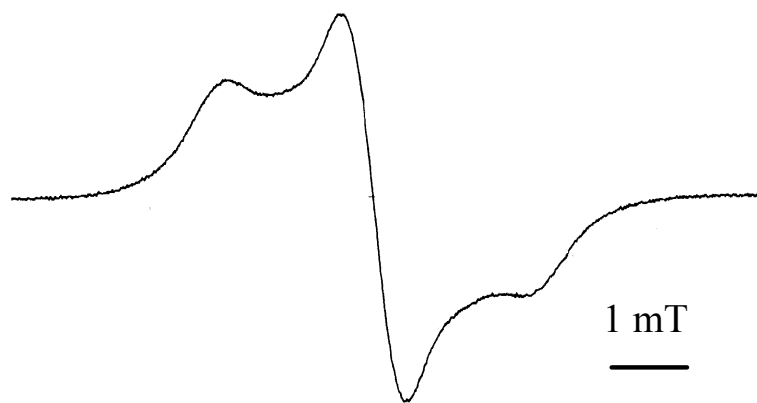
Sandberg, Sugawara *et al.*

Supplementary Information 4: Calculation of SOMOs of doubly protonated **QA** (**QA·H$_2$$^{2+}$**) based on the density functional theory.

The molecular orbitals of the dication diradical of **QA·H$_2$$^{2+}$** was calculated based on the density functional theory using a GAUSSIAN98 program package (UB3LYP/6-31G*//UB3LYP/6-31G*). The energy gap between the singlet and the triplet states was estimated to be 0.55 eV and the triplet state was calculated as the ground state. Coefficients of two SOMOs of **QA·H$_2$$^{2+}$** are shown below.

| SOMO	SOMO'
(HOMO)	(HOMO-1)
-0.357656 Hartree	-0.366546 Hartree

The distribution of coefficients of two SOMOs of doubly protonated **QA** (**QA·H$_2$$^{2+}$**) based on the density functional theory (B3LYP/6-31G*)
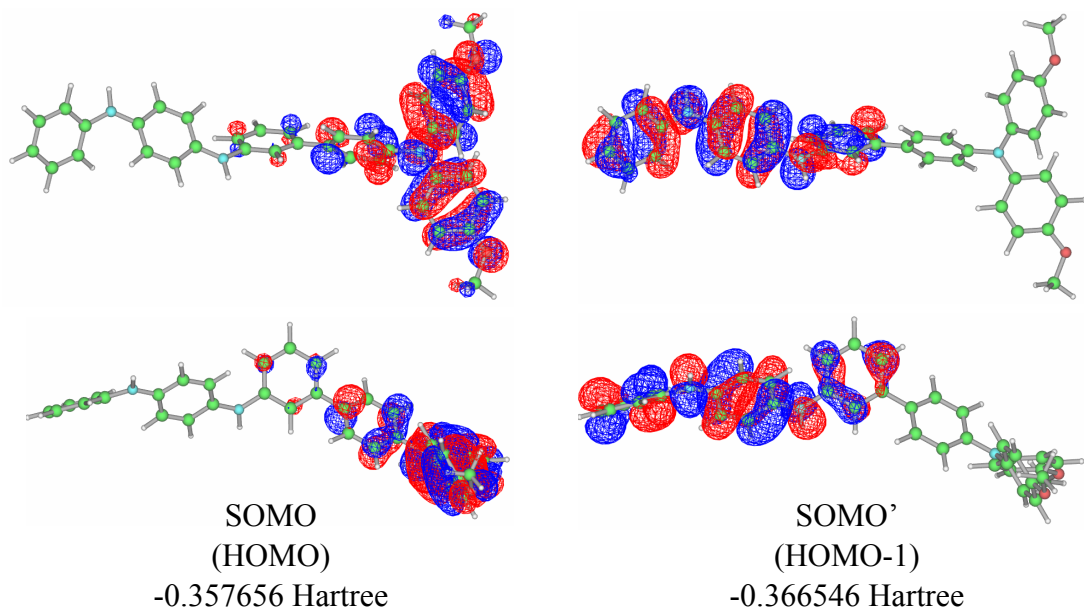
Sandberg, Sugawara *et al.*

Supplementary Information 5: Calculation of spin distribution of doubly protonated **QA** (**QA·H$_2$$^{2+}$**) based on the density functional theory and evaluation of the zero-field splitting parameter *D* value on the basis of the calculated spin distribution.

The spin density map of **QA·H$_2$$^{2+}$** calculated by the density functional theory (UB3LYP/6-31G*) shows that the spin densities distribute on the whole π-skeleton of the molecule.   The negative spin densities on several carbon atoms, are marked in red, exhibiting the spin-alternation.   The small *D* value of **QA**·H$_2$$^{2+}$ (*D*/hc = 0.0019 cm^{-1}) was well reproduced on the basis of a modified simple point-spin model (equation below) using the calculated spin distribution, although the theoretical equation for the *D* value of spin-distributed diradical is more complicated.   See: (a) Feller, D.; Borden, W. T.; Davidson, E. R. *J. Chem. Phys.* 1981, **74**, 2256.   (b) Hutton, R. S.; Roth, H. D. *J. Am. Chem. Soc.*, 1982, **104**, 1421.

View parpendicular to the phenyl ring in the middle

View parallel to the phenyl ring in the middle

Spin distribution of doubly protonated **QA·H$_2$$^{2+}$** based on the density functional theory (B3LYP/6-31G*)
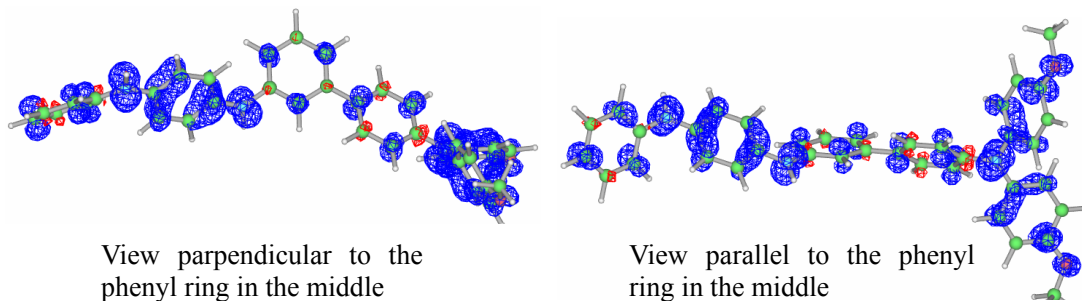
$$D/hc = \frac{3g\beta}{2} \sum_{i>j} \frac{\rho_i \cdot \rho_j}{|r_{ij}|^3} \qquad (\rho_i, \rho_j: \text{electron spin density})$$
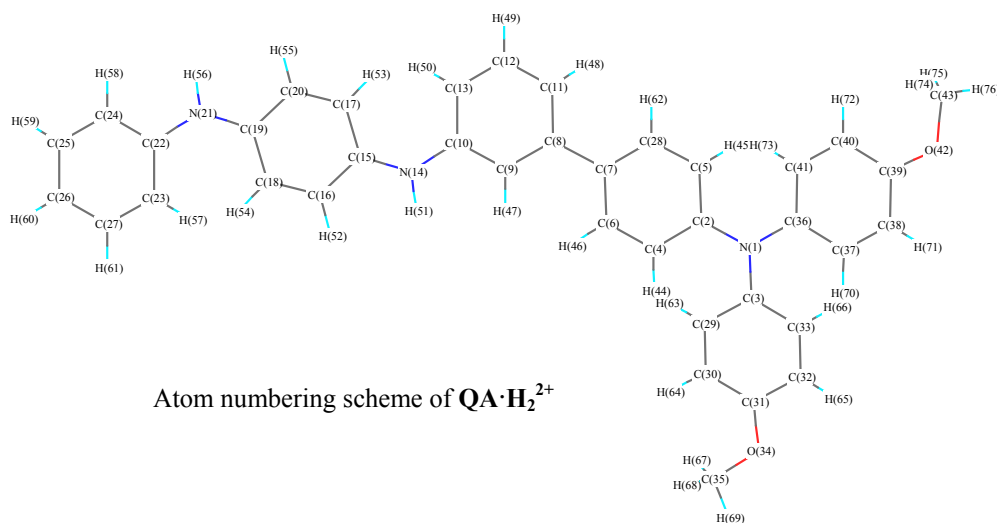

Atom numbering scheme of **QA·H$_2$$^{2+}$**

Table. Molecular conformation and spin densities of **QA·H$_2$$^{2+}$** by DFT calculation.

| Number	Atom	x	y	z	Spin Density
1	N	6.74934	0.89546	0.03606	0.30093
2	C	5.41231	1.35902	-0.03099	-0.046646
3	C	7.12221	-0.38593	0.56509	0.022699
4	C	4.30812	0.56601	0.38666	0.076736
5	C	5.11743	2.6785	-0.47914	0.076167
6	C	3.00577	1.0444	0.34996	-0.045217
7	C	2.72987	2.34143	-0.11841	0.0941
8	C	1.36583	2.85812	-0.14653	-0.041438
9	C	0.28468	1.99396	-0.35533	0.066033
10	C	-1.04538	2.47899	-0.34563	-0.039894
11	C	1.13478	4.23384	0.0426	0.073363
12	C	-0.16719	4.72589	0.00685	-0.036166
13	C	-1.26215	3.86134	-0.17998	0.067237
14	N	-2.06079	1.51476	-0.53433	0.188876
15	C	-3.44708	1.61977	-0.46371	0.126629
16	C	-4.20914	0.5108	-0.93538	0.016952
17	C	-4.15717	2.7289	0.06195	0.007728
18	C	-5.58449	0.55336	-0.98253	0.060953
19	C	-6.29953	1.6984	-0.53781	0.069114
20	C	-5.53468	2.77356	0.0293	0.071815
21	N	-7.67172	1.87167	-0.58687	0.268272
22	C	-8.69624	1.11655	-1.18485	-0.029152
23	C	-8.50293	-0.00418	-2.02219	0.081711
24	C	-10.02509	1.54094	-0.91374	0.082476
25	C	-11.10104	0.84827	-1.45429	-0.04532
26	C	-10.88889	-0.26828	-2.26897	0.114795
27	C	-9.60055	-0.67969	-2.5477	-0.044204
28	C	3.81009	3.14188	-0.52963	-0.045418
29	C	6.41339	-1.01579	1.61255	0.078293
30	C	6.8007	-2.25499	2.10455	-0.014869
31	C	7.92877	-2.89636	1.57292	0.105833
32	C	8.66081	-2.27385	0.53954	-0.019836
33	C	8.26852	-1.04997	0.0529	0.056145
34	O	8.42082	-4.11591	1.96671	0.058181
35	C	7.69817	-4.82886	2.95186	-0.004685
36	C	7.84654	1.68022	-0.46809	0.024568
37	C	9.09584	1.66255	0.19603	0.05666
38	C	10.16449	2.40829	-0.27064	-0.019679
39	C	10.04198	3.192	-1.43219	0.108288
40	C	8.7995	3.21222	-2.09589	-0.014459
41	C	7.73003	2.48599	-1.62314	0.079533
42	O	11.15047	3.89017	-1.8353	0.060102
43	C	11.1236	4.50073	-3.11275	-0.004833
44	H	4.43806	-0.47382	0.72556	-0.003328
45	H	5.89693	3.39061	-0.7943	-0.003282
46	H	2.18481	0.39655	0.69061	0.001949
47	H	0.49045	0.92461	-0.53011	-0.002495
48	H	1.97849	4.91818	0.20966	-0.003172
49	H	-0.34183	5.80429	0.11255	0.00171
50	H	-2.27275	4.2966	-0.17928	-0.003031
51	H	-1.72711	0.60356	-0.76138	-0.00833
52	H	-3.70235	-0.4044	-1.27768	-0.001477
53	H	-3.62459	3.58049	0.51277	-0.000824
54	H	-6.112	-0.32994	-1.37404	-0.002898
55	H	-6.0401	3.65303	0.45856	-0.003756
56	H	-8.0049	2.67915	-0.12203	-0.011651
57	H	-7.49989	-0.36469	-2.29468	-0.003813
58	H	-10.22739	2.41206	-0.27199	-0.0035
59	H	-12.12425	1.17915	-1.23637	0.001757
60	H	-11.7421	-0.81154	-2.69257	-0.005077
61	H	-9.44244	-1.5457	-3.20252	0.001928
62	H	3.62996	4.1646	-0.89401	0.001984
63	H	5.54622	-0.53502	2.09364	-0.003742
64	H	6.20277	-2.71136	2.90695	0.000305
65	H	9.54709	-2.77896	0.12997	0.000817
66	H	8.86879	-0.61902	-0.76367	-0.002733
67	H	6.67052	-5.02144	2.62564	0.003863
68	H	7.6991	-4.28777	3.9041	0.003935
69	H	8.25127	-5.7663	3.04465	-0.000022
70	H	9.24356	1.05739	1.10458	-0.002758
71	H	11.11652	2.36559	0.27713	0.000796
72	H	8.68568	3.80678	-3.01514	0.000265
73	H	6.78764	2.55551	-2.19028	-0.003812
74	H	10.33057	5.25543	-3.13341	0.003981
75	H	10.9781	3.7587	-3.90388	0.004059
76	H	12.10899	4.96355	-3.1943	-0.000021

Sandberg, Sugawara *et al.*

Supplementary Information 6: IR spectra of **QA** and **QA·H$_2$$^{2+}$** with their simulation data calculated by a DFT method.

The infrared spectra of **QA** and **QA·H$_2^{2+}$** (ClO$_4$ salt) were measured by an attenuated total-reflectance (ATR) method using Perkin-Elmer Spectrum One spectrometer equipped with a diamond ATR unit.   The measured data were corrected for the wavelength dependence of ATR absorption.   These experimental data were well reproduced by a DFT calculation (B3LYP/6-31G*).

Sandberg, Sugawara *et al.*

Supplementary Information 7: Comparison of IR spectra of **QA·H$_2$$^{2+}$** and the annealed one.
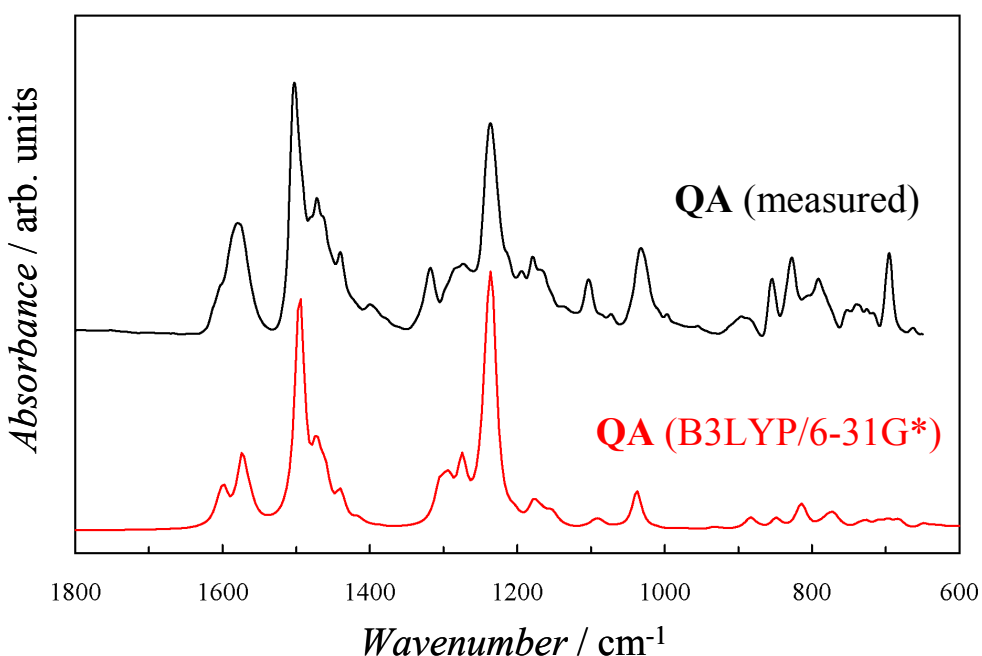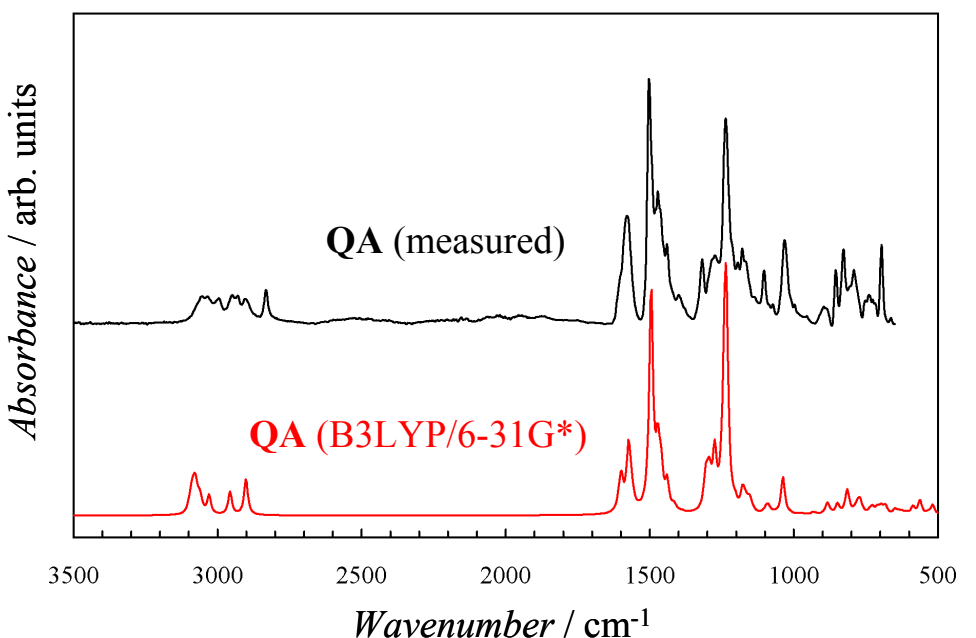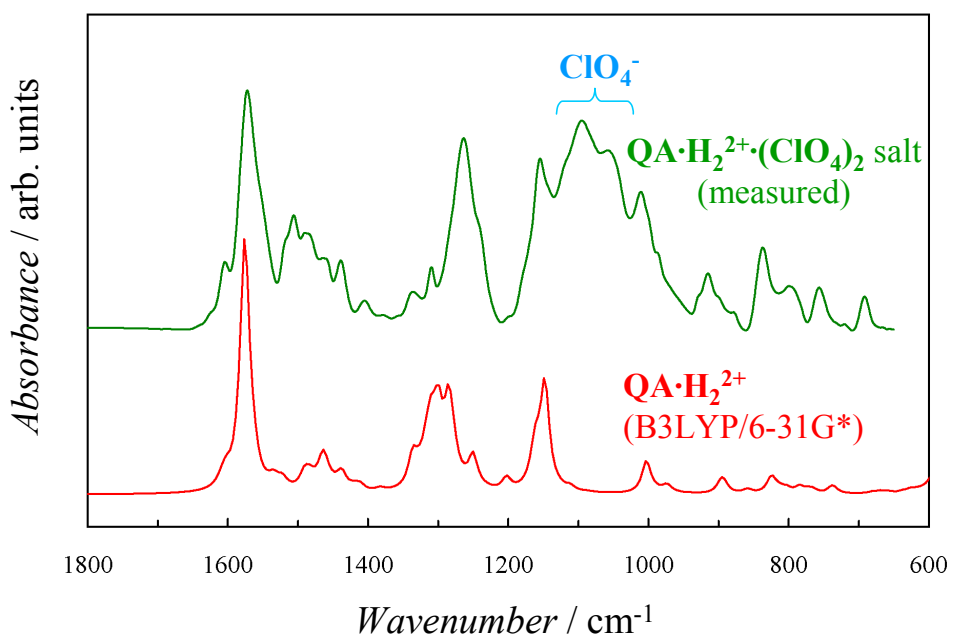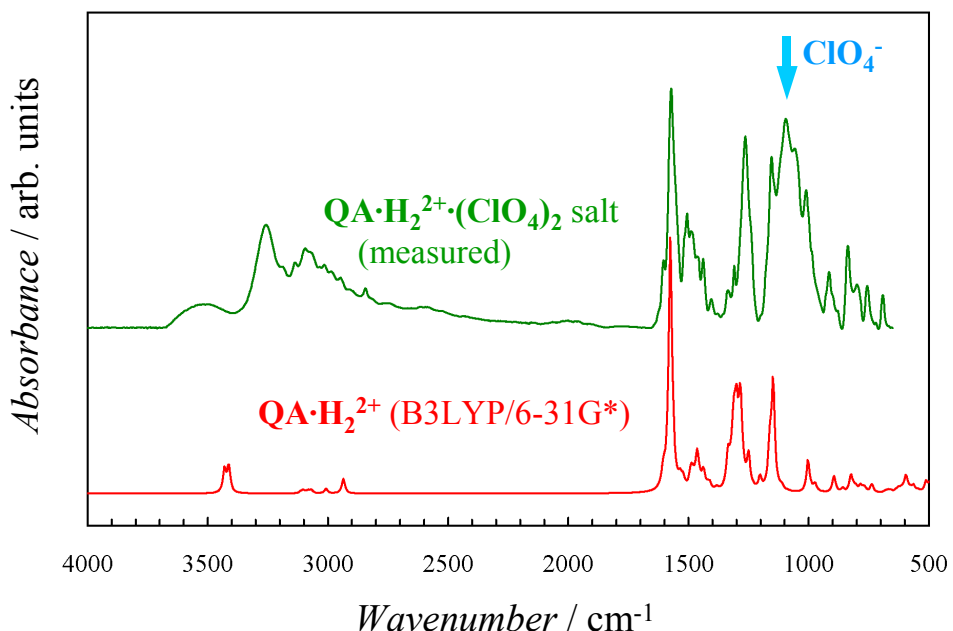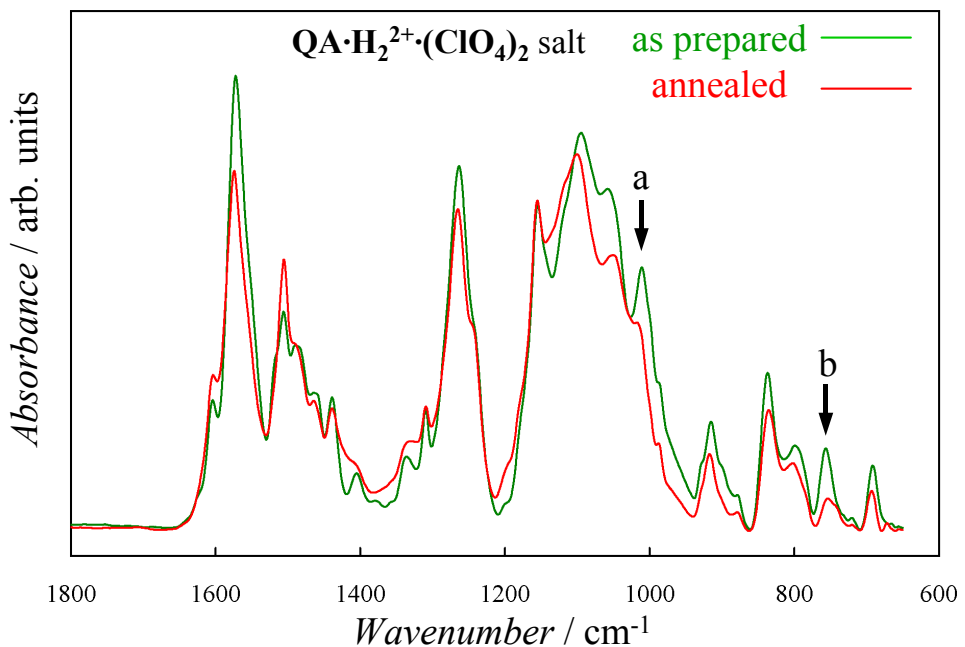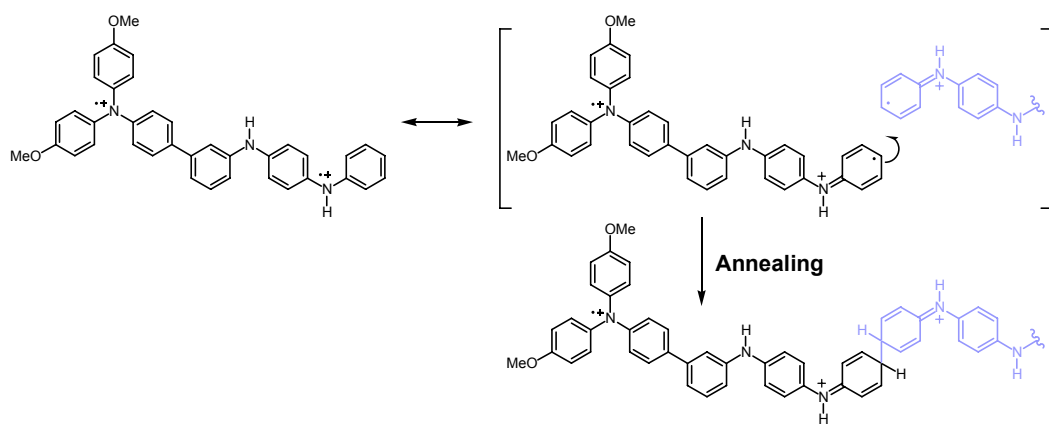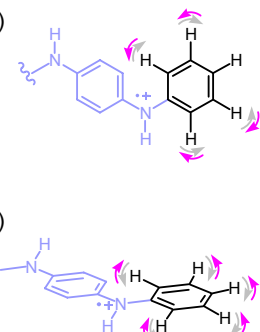
After annealing at 400 K, the IR spectrum of **QA·H$_2$$^{2+}$·(ClO$_4$)$_2$** salt (a) changed from that of the fresh sample. Two peaks indicated by arrows showe the largest difference in comparison with the fresh sample. These peaks were assigned as (a) in plane bending and (b) out of plane bending modes of C-H bonds of phenyl ring at the edge of molecule in reference to the theoretical calculation (B3LYP/6-31G*). This result suggests that (b) the decrease of Curie constant in the annealed sample comes from the chemical bond formation with adjacent molecule at the para-position of phenyl ring where has large electron spin density.

Scheme. A plausible mechanism for radical quenching of **QA·H$_2$$^{2+}$·(ClO$_4$)$_2$** salt upon annealing.